

Time exponentiation of a Wilson loop for Yang-Mills theories in 2 + ϵ dimensions

A. Bassetto

Dipartimento di Fisica “G. Galilei”, Via Marzolo 8, 35131 Padova, Italy

INFN, Sezione di Padova, Italy

R. Begliuomini and G. Nardelli

Dipartimento di Fisica, Università di Trento, 38050 Povo (Trento), Italy

INFN, Gruppo Collegato di Trento, Italy

Abstract

A rectangular Wilson loop centered at the origin, with sides parallel to space and time directions and length $2L$ and $2T$ respectively, is perturbatively evaluated $\mathcal{O}(g^4)$ in Feynman gauge for Yang–Mills theory in $1+(D-1)$ dimensions. When $D > 2$, there is a dependence on the dimensionless ratio L/T , besides the area. In the limit $T \rightarrow \infty$, keeping $D > 2$, the leading expression of the loop involves only the Casimir constant C_F of the fundamental representation and is thereby in agreement with the expected Abelian-like time exponentiation (ALTE). At $D = 2$ the result depends also on C_A , the Casimir constant of the adjoint representation and a pure area law behavior is recovered, but no agreement with ALTE in the limit $T \rightarrow \infty$. Consequences of these results concerning two and higher-dimensional gauge theories are pointed out.

Padova preprint DFPD 98/TH/32; PACS: 11.10 Kk, 12.38 Bx

keywords: Perturbative Wilson loop calculation; QCD in lower dimensions

I. INTRODUCTION

There are several reasons why $SU(N)$ Yang-Mills (YM) theories are interesting in 1+1 dimensions. First of all, this reduction entails tremendous simplifications, so that many problems can be faced, and often solved, even beyond perturbation theory. We are referring to exact evaluations of vacuum to vacuum amplitudes of Wilson loop operators, that, for a suitable choice of contour and in a particular limit, provide the potential between a static $q\bar{q}$ pair [1], [2], [3].

Another celebrated example is the spectrum of $q\bar{q}$ bound states in the large- N limit, when dynamical fermions are also taken into account [4].

In 1+1 dimensions YM theories without fermions are considered free theories, apart from topological effects. This feature looks apparent when choosing an axial gauge. However they exhibit severe infrared (IR) divergences, which need to be regularized. In ref. [4] an explicit IR cutoff is advocated, which turns out to be unimportant on the bound state spectrum; a Cauchy principal value (CPV) prescription in handling the IR singularity in the gluon propagator leads indeed to the same result [5]. On the other hand this prescription emerges quite naturally if the theory is quantized at “equal x^+ ”, namely adopting the light-front $x^+ = 0$ as quantization surface.

Still difficulties in performing a Wick’s rotation in the dynamical equations was pointed out in ref. [6]. In order to remedy such a situation, a causal prescription for the double pole in the kernel was proposed, which is nothing but the one suggested years later by Mandelstam and Leibbrandt (ML) [7], when restricted to 1+1 dimensions. This prescription follows from equal-time quantization [8] and is mandatory in order to renormalize the theory in 1+3 dimensions [9], [10].

In view of the above-mentioned results and of the fact that “pure” YM theory does not immediately look free in Feynman gauge, a test of gauge invariance was performed in ref. [11] by calculating at $\mathcal{O}(g^4)$, both in Feynman and in light-cone gauge with ML prescription, a rectangular Wilson loop with light-like sides, directed along the vectors $n_\mu = (T, -T)$,

$n_\mu^* = (L, L)$ and parametrized according to the equations:

$$\begin{aligned}
C_1 : x^\mu(t) &= n^{*\mu} t, \\
C_2 : x^\mu(t) &= n^{*\mu} + n^\mu t, \\
C_3 : x^\mu(t) &= n^\mu + n^{*\mu}(1-t), \\
C_4 : x^\mu(t) &= n^\mu(1-t), \quad 0 \leq t \leq 1.
\end{aligned} \tag{1}$$

This contour has been considered in refs. [12,13] for an analogous test of gauge invariance in 1+3 dimensions. Its light-like character forces a Minkowski treatment.

In order to perform the test, dimensional regularization was used; the Feynman gauge option is indeed not viable at strictly 1+1 dimensions, as the usual free vector propagator is not a tempered distribution.

The following unexpected results were obtained.

The $\mathcal{O}(g^4)$ perturbative loop expression in $d = 1 + (D - 1)$ dimensions is finite in the limit $D \rightarrow 2$. The results in the two gauges coincide, as required by gauge invariance. They are function only of the area $n \cdot n^*$ for any dimension D and exhibit also a dependence on C_A , the Casimir constant of the adjoint representation.

This dependence, when looked at in the light-cone gauge calculation, comes from non-planar diagrams with the colour factor $C_F(C_F - C_A/2)$, C_F being the Casimir constant of the fundamental representation. Besides, there is a genuine contribution proportional to $C_F C_A$ coming from the one-loop correction to the vector propagator. This is surprising at first sight, as in strictly 1+1 dimensions the triple vector vertex vanishes in axial gauges. What happens is that transverse degrees of freedom, although coupled with a vanishing strength at $D = 2$, produce finite contributions when matching with the self-energy loop singularity precisely at $D = 2$, eventually producing a finite result. Such a phenomenon could not appear in a strictly 1+1 dimensional calculation, which would only lead to the (smooth) non-planar diagram result. We stress that this contribution is essential to get agreement with the Feynman gauge calculation, in other words with gauge invariance.

We notice that no ambiguity affects our light-cone gauge results, which do not involve

infinities; in addition the discrepancy cannot be accounted for by a simple redefinition of the coupling, that would also, while unjustified on general grounds, turn out to be dependent on the area of the loop.

In order to make the argument complete, we recall that a calculation of the same Wilson loop in strictly 1+1 dimension in light-cone gauge with a CPV prescription for the “spurious” singularity produces a vanishing contribution from non-planar graphs. Only planar diagrams survive, leading to Abelian-like results depending only on C_F , which can be resummed to all orders in the perturbative expansion to recover the expected exponentiation of the area.

This result, which is the usual one found in the literature, although quite transparent, *does not coincide* with the Feynman gauge result in the limit $D \rightarrow 2$ [11].

The test cannot be generalized to $D \neq 2$ dimensions as CPV prescription is at odd with causality in this case [10].

In order to clarify whether there is indeed a pathology in the light-cone gauge formulation with ML prescription in strictly 1+1 dimensions, one can try to study the potential $V(2L)$ between a “static” $q\bar{q}$ pair in the fundamental representation, separated by a distance $2L$. Then a different Wilson loop is to be considered, *viz* a rectangular loop with one side along the space direction and one side along the time direction, of length $2L$ and $2T$ respectively. Eventually the limit $T \rightarrow \infty$ at fixed L is to be taken: the potential $V(2L)$ between the quark and the antiquark is indeed related to the value of the corresponding Wilson loop amplitude $\mathcal{W}(L, T)$ through the Abelian-like time exponentiation (ALTE) formula [14]

$$\lim_{T \rightarrow \infty} \mathcal{W}(L, T) = \text{const. } e^{-2iT V(2L)} . \quad (2)$$

We remark that this condition is stronger than requiring [2]

$$\lim_{T \rightarrow \infty} \frac{1}{T} \log \mathcal{W}(L, T) = \text{const.} ,$$

which, for instance, allows T -dependent polynomials factors.

The crucial point to notice in eq.(2) is that dependence on the Casimir constant C_A should cancel at the leading order when $T \rightarrow \infty$ in any coefficient of a perturbative expansion of

the potential with respect to coupling constant. This criterion has often been used as a check of gauge invariance [10].

The study of this Wilson loop in strictly 1+1 dimensions has been performed in light-cone gauge [15]. In the CPV case, due to its essentially Abelian nature, the loop can be exactly evaluated and a simple exponentiation of the area is recovered, thus providing a linear potential between the quark and the antiquark. In particular only the Casimir constant C_F appears.

The corresponding calculation in the ML case develops genuine non-Abelian terms proportional to C_A ; thus, contrary to the previous case, the loop interaction feels the non-Abelian nature of the theory. The loop still depends only on the area, but ALTE is lost: in the limit $T \rightarrow \infty$ a dependence on C_A survives [15], [16].

Although ALTE can be proven only introducing the “true spectrum” of the theory, which is beyond the perturbative regime, we feel somehow uneasy with this conclusion, which is at variance with all the previous tests of gauge invariance considered in the literature. We are thereby led to consider this phenomenon as a peculiarity of strictly two-dimensional theories, which occurs when topological excitations are disregarded as in perturbative loop calculations.

Then the interest arises in performing the same Wilson loop calculation in dimensions $D > 2$. It may indeed happen that the limits $T \rightarrow \infty$ and $D \rightarrow 2$ do not commute.

The main result of this paper, namely that, in the large T -limit when $D > 2$, the perturbative $\mathcal{O}(g^4)$ contribution is in agreement with ALTE, supports the conclusion above.

Owing to the very heavy character of the calculation, we choose to work in Feynman gauge. In Sect.2 we review basic concepts and notation. We also compute the Wilson loop at $\mathcal{O}(g^2)$. In Sect.3 the relevant diagrams at $\mathcal{O}(g^4)$ are computed in $D = 2\omega$ dimensions, after collecting them in three basic families, the “exchange” diagrams, the “self-energy” and the “spider” ones, namely those involving the triple vector vertex. For $D > 2$ the loop depends, besides on the area, also on the ratio $\beta = L/T$. As we are eventually interested in

the large- T behavior, we shall always consider the region $\beta < 1$; moreover we shall choose $\omega = 1 + \epsilon$, with a small, positive ϵ . Sect.4 contains our conclusions. In it we show that, when $D > 2$, agreement with ALTE occurs in the limit $T \rightarrow \infty$, with a pure C_F -dependence in the leading coefficient. Agreement with all previous results [10] in higher dimensions is thus re-established.

To perform instead the limit $D \rightarrow 2$ for generic values of β in a rigorous way, turns out to be extremely difficult from a technical viewpoint. As a matter of fact the contribution coming from graphs with the triple gluon vertex, exhibits quite involved analyticity properties in the variable β . Nevertheless, if such a limit is performed accepting a natural conjecture we shall explain later on, the result one gets exactly coincides with the gauge invariant one obtained in ref. [11] for a loop of the same area with light-like sides; thereby we enforce the argument that in two dimensions a pure area behavior is to be expected, no matter the orientation and the shape of the loop. In so doing, however, in two dimensions at $\mathcal{O}(g^4)$ a C_A -dependence is definitely there and there is no agreement with ALTE.

The theory looks indeed discontinuous in the limit $D \rightarrow 2$.

Details of the calculations are given in the Appendices.

II. GENERAL CONSIDERATIONS

We consider the usual “gauge fixed” Yang-Mills Lagrangian,

$$\mathcal{L} = -\frac{1}{4}F_{\mu\nu}^a F^{a\mu\nu} + \frac{1}{2}\partial^\mu A_\mu^a \partial^\nu A_\nu^a. \quad (3)$$

Without loss of generality, we consider $SU(N)$ as gauge group, so that the field strength in (3) is defined as $F_{\mu\nu}^a = \partial_\mu A_\nu^a - \partial_\nu A_\mu^a + g f^{abc} A_\mu^b A_\nu^c$, f^{abc} being the structure constants of $SU(N)$.

We consider the closed path γ parametrized by the following four segments γ_i ,

$$\gamma_1 : \gamma_1^\mu(s) = (sT, L) ,$$

$$\gamma_2 : \gamma_2^\mu(s) = (T, -sL) ,$$

$$\begin{aligned}\gamma_3 : \gamma_3^\mu(s) &= (-sT, -L) , \\ \gamma_4 : \gamma_4^\mu(s) &= (-T, sL) , \quad -1 \leq s \leq 1.\end{aligned}\tag{4}$$

describing a (counterclockwise-oriented) rectangle centered at the origin of the plane (x^1, x^0) , with length sides $(2L, 2T)$, respectively (see Fig. 1). Then, for the definition of the Wilson loop around γ we shall adopt the standard one, given by the following vacuum to vacuum amplitude

$$\mathcal{W}_\gamma(L, T) = \frac{1}{N} \langle 0 | \text{Tr} \left[\mathcal{T} \mathcal{P} \exp \left(ig \oint_\gamma dx^\mu A_\mu^a(x) T^a \right) \right] | 0 \rangle , \tag{5}$$

where \mathcal{T} orders gauge fields in time and \mathcal{P} orders generators T^a of the gauge group $SU(N)$ along the closed integration path γ . The perturbative expansion of the Wilson loop (5) looks like

$$\mathcal{W}_\gamma(L, T) = 1 + \frac{1}{N} \sum_{n=2}^{\infty} (ig)^n \oint_\gamma dx_1^{\mu_1} \cdots \oint_\gamma dx_n^{\mu_n} \theta(x_1 > \cdots > x_n) \text{Tr}[G_{\mu_1 \cdots \mu_n}(x_1, \dots, x_n)] , \tag{6}$$

where $G_{\mu_1 \cdots \mu_n}(x_1, \dots, x_n)$ is the Lie algebra valued n -point Green function, in which further dependence on the coupling constant is usually buried; the Heavyside θ -functions order the points x_1, \dots, x_n along the integration path γ .

It is easy to show that the perturbative expansion of \mathcal{W}_γ is an even power series in the coupling constant, so that we can write

$$\mathcal{W}_\gamma(L, T) = 1 + g^2 \mathcal{W}_2 + g^4 \mathcal{W}_4 + \mathcal{O}(g^6) . \tag{7}$$

An explicit evaluation of the function \mathcal{W}_2 in eq. (7) gives the diagrams contributing to the loop with a single exchange (i.e. one propagator), namely

$$\mathcal{W}_2 = -\frac{1}{2} C_F \oint \oint D_{\mu\nu}(x - y) dx^\mu dy^\nu , \tag{8}$$

where $D_{\mu\nu}(x)$ is the usual free propagator in Feynman gauge

$$D_{\mu\nu}(x) = -g_{\mu\nu} \frac{\pi^{-D/2}}{4} \Gamma(D/2 - 1) (-x^2 + i\epsilon)^{1-D/2}.$$

A fairly easy calculation leads to the result

$$\begin{aligned} \mathcal{W}_2 = & \frac{C_F}{\pi^\omega} (2L)^{2-2\omega} LT \left[i\Gamma(\omega - 3/2)\Gamma(1/2) \right. \\ & \left. + \frac{2\beta\Gamma(\omega)}{\omega - 2} \left(\frac{1}{3 - 2\omega} - e^{-i\pi\omega} \sum_{n=1}^{\infty} \frac{\Gamma(n + \omega - 2)}{\Gamma(\omega - 2)} \frac{\beta^{2n+2\omega-4}}{(2n-1)(2n+2\omega-3)n!} \right) \right]. \end{aligned} \quad (9)$$

It should be noticed that this result does not coincide with the corresponding one in ref. [11], which was evaluated in the same gauge choice but with the loop sides along the x^+ and x^- directions. Contrary to what happens in ref. [11], eq. (9) exhibits an explicit dependence on the ratio $\beta = L/T$. Only in the two dimensional limit the two results coincide: the limit $\omega \rightarrow 1$ is smooth and gives the pure area dependence

$$\mathcal{W}_2 = -2iC_F LT.$$

The diagrams contributing to \mathcal{W}_4 can be grouped into three distinct families

$$\mathcal{W}_4 = \mathcal{W}^{(1)} + \mathcal{W}^{(2)} + \mathcal{W}^{(3)}:$$

- the ones with a double gluon exchange in which the propagators can either cross or uncross;
- the ones in which the gluon propagator contains a self-energy correction;
- the ones involving a triple vector coupling.

In strictly two dimensions and in an axial gauge only the first family is present. In Feynman gauge all of them must be taken into account; moreover we are here considering the problem in D-dimensions. The first family is also the only one contributing to the Abelian case.

III. WILSON LOOP CALCULATIONS

We start by considering the diagrams belonging to the first category: a straightforward calculation gives

$$\mathcal{W}^{(1)} = \frac{1}{8N} \oint \oint \oint \oint \text{Tr}[\mathcal{P}(T_x^a T_y^a T_z^b T_w^b)] D_{\mu\nu}(x - y) D_{\rho\sigma}(z - w) dx^\mu dy^\nu dz^\rho dw^\sigma , \quad (10)$$

where subscripts in the matrices have been introduced to specify their ordering. From eq. (10), the diagrams with two-gluons exchanges contributing to the order g^4 in the perturbative expansion of the Wilson loop fall into two distinct classes, depending on the topology of the diagrams:

1. *Non-crossed diagrams*: if the pairs (x, y) and (z, w) are contiguous around the loop the two propagators do not cross (see Fig. 2a) and the trace in (10) gives $\text{Tr}[T^a T^a T^b T^b] = NC_F^2$.
2. *Crossed diagrams*: if the pairs (x, y) and (z, w) are not contiguous around the loop the two propagators do cross (see Fig. 2b) and the trace in (10) gives $\text{Tr}[T^a T^b T^a T^b] = \text{Tr}[T^a (T^a T^b + [T^b, T^a]) T^b] = N(C_F^2 - (1/2)C_A C_F)$, C_A being the Casimir constant of the adjoint representation defined by $f^{abc} f^{dbc} = C_A \delta^{ad}$.

We see that the C_F^2 term is present in both types of diagrams and with the same coefficient. This term is usually denoted “Abelian term”: were the theory Abelian, only such C_F^2 terms would contribute to the loop. On the other hand, the $C_F C_A$ term is present only in crossed diagrams, and is typical of non-Abelian theories.

Thus, we can decompose $\mathcal{W}^{(1)}$ as the sum of an Abelian and a non-Abelian part,

$$\mathcal{W}^{(1)} = \mathcal{W}_{ab} + \mathcal{W}_{na} . \quad (11)$$

Moreover, the Abelian part is simply half of the square of the order- g^2 term, i.e.

$$\begin{aligned} \mathcal{W}_{ab} &= \frac{1}{8} C_F^2 \oint \oint \oint \oint D_{\mu\nu}(x - y) D_{\rho\sigma}(z - w) dx^\mu dy^\nu dz^\rho dw^\sigma \\ &= \frac{1}{2} \left(-\frac{1}{2} C_F \oint \oint D_{\mu\nu}(x - y) dx^\mu dy^\nu \right)^2 . \end{aligned} \quad (12)$$

Equation (12) is just a particular case of a more general theorem due to Frenkel and Taylor [17], which proves that the only relevant terms in the perturbative expansion of the loop are the so-called “maximally non-Abelian” ones; at $\mathcal{O}(g^4)$ those terms are just proportional to $C_F C_A$. They are the only ones we have to evaluate to get \mathcal{W}_{na} .

All the Abelian terms (depending only on C_F) in the perturbative expansion of the Wilson loop sum up to reproduce the Abelian exponential

$$\mathcal{W}_\gamma^{ab}(L, T) = \exp \left(-\frac{1}{2} C_F g^2 \oint \oint D_{\mu\nu}(x - y) dx^\mu dy^\nu \right) , \quad (13)$$

where the result in eq.(9) can be introduced. This result at $\mathcal{O}(g^4)$ has been explicitly checked calculating the relevant non-crossed exchange diagrams (see Appendix A for details).

In the limit $D \rightarrow 2$ the simple exponentiation of the area is easily recovered

$$\mathcal{W}_\gamma^{ab}(L, T) = \exp \left[-\frac{i}{2} C_F g^2 \mathcal{A} \right] , \quad (14)$$

where $\mathcal{A} = 4LT$ is the area of the loop.

We have now to calculate loop integrals of the type given in eq.(10). In view of the parametrization (4), it is convenient to decompose loop integrals as sums of integrals over the segments γ_i , and to this purpose we define

$$E_{ij}(s, t) = D_{\mu\nu}[\gamma_i(s) - \gamma_j(t)] \dot{\gamma}_i^\mu(s) \dot{\gamma}_j^\nu(t) , \quad i, j = 1, \dots, 4 , \quad (15)$$

where the dot denotes the derivative with respect to the variable parametrizing the segment. In this way, each diagram can be written as integrals of products of functions of the type (15). Each graph will be labelled by a set of pairs (i, j) , each pair denoting a gluon propagator joining the segments γ_i and γ_j .

Due to the symmetric choice of the contour γ and to the fact that propagators are even functions, i.e. $D_{\mu\nu}(x) = D_{\mu\nu}(-x)$, we have the following identities that halve the number of diagrams to be evaluated:

$$\begin{aligned} E_{ij}(s, t) &= E_{ji}(t, s) , \\ E_{11}(s, t) &= E_{33}(s, t) , \\ E_{22}(s, t) &= E_{44}(s, t) . \end{aligned} \quad (16)$$

We remind the reader that in Feynman gauge the propagators can attach either to the same rectangle side or to opposite sides, but not on a couple of contiguous ones.

We have now to consider the $\mathcal{O}(g^4)$ $C_F C_A$ -terms. From the previous discussion it follows that only “crossed diagrams” (maximally non-Abelian ones) need to be evaluated

$$\begin{aligned}\mathcal{W}_{na} &= -\frac{1}{2} C_A C_F \sum_{i,j,k,l} ' \int ds \int dt \int du \int dv E_{ij}(s,t) E_{kl}(u,v) \\ &\equiv -\frac{1}{2} C_A C_F \sum_{i,j,k,l} ' C_{(ij)(kl)} ,\end{aligned}\tag{17}$$

where the primes mean that we have to sum only over crossed propagators configurations and over topologically inequivalent contributions, as carefully explained in the following; we have not specified the integration extrema as they depend on the particular type of crossed diagram we are considering (the extrema must be chosen in such a way that propagators remain crossed).

The last equality in eq. (17) defines the general diagram $C_{(ij)(kl)}$: it is a diagram with two *crossed* propagators joining the sides (ij) and (kl) of the contour (4). In Fig. 3 a few examples of diagrams are drawn to get the reader acquainted with the notation. The first of eq. (16) permits to select just 11 types of topologically distinct crossed diagrams. The remaining symmetry relations (16) further lower the number to 7. As a matter of fact, although topologically inequivalent, from eq. (16) it is easy to get

$$\begin{aligned}C_{(11)(11)} &= C_{(33)(33)} , & C_{(22)(22)} &= C_{(44)(44)} , \\ C_{(11)(13)} &= C_{(33)(13)} , & C_{(22)(24)} &= C_{(44)(24)} .\end{aligned}\tag{18}$$

which are the 4 relations needed to lower the number of diagrams to be evaluated from 11 to 7. Besides the 8 diagrams quoted in eq. (18), there are three other crossed diagrams that do not possess any apparent symmetry relation with other diagrams: $C_{(13)(13)}$, $C_{(24)(24)}$ and $C_{(13)(24)}$ (see Fig. 4), so that the number of topologically inequivalent crossed diagrams is indeed 11.

The calculation of the 7 independent diagrams needed is lengthy and not trivial. The details of such calculation are reported in Appendix A. Each diagram depends not only on the area $A = 4LT$ of the loop, but also on the dimensionless ratio $\beta = L/T$ through complicated multiple integrals involving powers depending on ω .

Adding all the contributions as in eq. (17) we eventually arrive at the following result $\mathcal{O}(g^4)$ for the non-Abelian part of the exchange diagrams contribution:

$$\begin{aligned}\mathcal{W}_{na} &= C_F C_A \frac{(2T)^{4-4\omega}}{\pi^{2\omega}} (LT)^2 e^{-2i\pi\omega} \\ &\times \left(\frac{\Gamma^2(\omega-1)}{(2\omega-4)(2\omega-3)} \left[1 + \frac{1-\omega}{(4\omega-5)(2\omega-3)} + \mathcal{O}(\beta^{5-4\omega}) \right] \right).\end{aligned}\quad (19)$$

We notice that the expression above exhibits a double and a single pole at $\omega = 1$, whose Laurent expansion gives

$$\frac{\mathcal{W}_{na} \pi^{2\omega} e^{2i\pi\omega}}{C_F C_A (2T)^{4-4\omega} (LT)^2} = \frac{1}{2(\omega-1)^2} + \frac{1-\gamma}{(\omega-1)} - 1 - 2\gamma + \gamma^2 + \frac{\pi^2}{12} + \mathcal{O}(\omega-1), \quad (20)$$

γ being the Euler-Mascheroni constant.

We turn now our attention to the calculation of $\mathcal{W}^{(2)}$, namely of the diagrams with a single gluon exchange in which the propagator contains a self-energy correction $\mathcal{O}(g^2)$. Of course both gluon and ghost contribute to the self-energy. The color factor is obviously a pure $C_F C_A$.

We call them “bubble” diagrams. We denote by B_{ij} the contribution of the diagram in which the propagator connects the rectangle segments γ_i, γ_j (see Fig. 5).

There are 10 topologically inequivalent diagrams; however, the symmetries we have already discussed and the symmetric choice of the contour entails the four conditions $B_{11} = B_{33}$, $B_{22} = B_{44}$, $B_{12} = B_{34}$, $B_{14} = B_{23}$, whereas the remaining two diagrams B_{13} and B_{24} are unrelated by any symmetry relation. In addition, it is easy to see by performing a simple change of variable that B_{14} and B_{34} are equal. Thus, there are 5 independent diagrams to be evaluated

$$\mathcal{W}^{(2)} = B_{13} + B_{24} + 2B_{11} + 2B_{22} + 4B_{12}. \quad (21)$$

The details of the calculation are described in Appendix B. We here report the final result in the form of an expansion with respect to the variable β

$$\mathcal{W}^{(2)} = C_F C_A \frac{(2T)^{4-4\omega}}{\pi^{2\omega}} (LT)^2 e^{-2i\pi\omega} \times \begin{aligned} & \left[\frac{(3\omega-1)\Gamma^2(\omega)}{2\Gamma(2\omega)\Gamma(4-\omega)} \Gamma(1-\omega)\Gamma(2\omega-2) \left(\frac{2\omega-6}{5-4\omega} + \mathcal{O}(\beta^{5-4\omega}) \right) \right]. \end{aligned} \quad (22)$$

Again we notice the presence of a double and of a single pole at $\omega = 1$. The relevant Laurent expansion is

$$\frac{\mathcal{W}^{(2)} \pi^{2\omega} e^{2i\pi\omega}}{C_F C_A (2T)^{4-4\omega} (LT)^2} = \frac{1}{(\omega-1)^2} + \frac{9-4\gamma}{2(\omega-1)} + \frac{39}{2} - 9\gamma + 2\gamma^2 + \frac{\pi^2}{6} + \mathcal{O}(\omega-1), \quad (23)$$

The third quantity $\mathcal{W}^{(3)}$ is by far the most difficult one to be evaluated. It comes from “spider” diagrams, namely the diagrams containing the triple gluon vertex (see Fig. 6). We denote by S_{ijk} the contribution of the diagram in which the propagators are attached to the segments $\gamma_i, \gamma_j, \gamma_k$.

It can be checked that all the spiders with the three legs attached to the same line vanish, as well as the spiders with two legs on one side and the third leg attached to the opposite side, *i.e.* $S_{111} = S_{222} = S_{333} = S_{444} = S_{113} = S_{133} = S_{224} = S_{244} = 0$. Thus, there are 12 non-vanishing topologically inequivalent diagrams; however, their number is just halved by the symmetric choice of the contour ($S_{124} = S_{234}, S_{123} = S_{134}, S_{112} = S_{334}, S_{233} = S_{114}, S_{344} = S_{122}, S_{144} = S_{223}$), so that $\mathcal{W}^{(3)}$ can be expressed in terms of the remaining 6 independent ones

$$\mathcal{W}^{(3)} = 2S_{112} + 2S_{123} + 2S_{124} + 2S_{233} + 2S_{144} + 2S_{344}. \quad (24)$$

Each term is represented by a multiple integral which cannot be evaluated for a generic dimension ω in closed form. In particular it exhibits complicated analyticity properties in the variable β , just in the neighborhood of the value $\beta = 0$ which is of interest for us. Details of the calculation are again deferred to an Appendix (Appendix C).

We have succeeded in obtaining the following result for $D > 2$

$$\lim_{\beta \rightarrow 0} \frac{\mathcal{W}^{(3)} \pi^{2\omega} e^{2i\pi\omega}}{C_F C_A (2T)^{4-4\omega} (LT)^2} = -\frac{3}{2(\omega-1)^2} + \frac{3\gamma - 11/2}{(\omega-1)} - \frac{35}{2} + 11\gamma - 3\gamma^2 + \frac{\pi^2}{12} + \mathcal{O}(\omega-1). \quad (25)$$

A double and a single pole at $D = 2$ again are present in this expression.

IV. CONCLUDING REMARKS

Since the Abelian part of our results depends only on the Casimir constant C_F and smoothly exponentiates in the large- T limit even when $D > 2$ (see eqs.(9,13)), in the following we focus our attention on the non-Abelian part, namely on the quantity containing the factor $C_F C_A$

$$\mathcal{W}_{na} + \mathcal{W}^{(2)} + \mathcal{W}^{(3)}.$$

It is actually convenient to divide by the square of the loop area, by introducing the new expression \mathcal{N}

$$\mathcal{N} C_F C_A (LT)^2 = \mathcal{W}_{na} + \mathcal{W}^{(2)} + \mathcal{W}^{(3)}. \quad (26)$$

Then, from eqs.(19,22,25), it is easy to conclude that, thanks to the factor $T^{4-4\omega}$, \mathcal{N} vanishes in the limit $T \rightarrow \infty$ when $\omega > 1$.

This is precisely the usual necessary condition required at $\mathcal{O}(g^4)$ in order to get agreement with ALTE when summing higher orders [10].

We cannot discuss the limit $\omega \rightarrow 1$ for generic (small) values of β in our results as we are only able to master the expressions at $\beta = 0$.

Nevertheless if we consider the quantity

$$\lim_{\omega \rightarrow 1} \lim_{\beta \rightarrow 0} (T^{4\omega-4} \mathcal{N})$$

we get a quite interesting result. Indeed double and simple poles at $\omega = 1$ cancel in the sum, leading to

$$\lim_{\omega \rightarrow 1} \lim_{\beta \rightarrow 0} (T^{4\omega-4} \mathcal{N}) = \frac{1}{\pi^2} \left(1 + \frac{\pi^2}{3}\right), \quad (27)$$

which *exactly* coincides with eq.(13) of [11].

This is, first of all, a formidable check of all our calculations, if we conjecture that the same result is obtained by performing the limit

$$\lim_{\beta \rightarrow 0} \lim_{\omega \rightarrow 1} \mathcal{N}.$$

But it also entails the quite non trivial consequences we are going to discuss.

At a first sight one could have thought to recover the result obtained in strictly 1+1 dimensions in ref. [15]. This is not the case; as a matter of fact in strictly 1+1 dimensions and in light-cone gauge the contribution from diagrams containing a self-energy insertion is missing, in spite of the fact that, if calculated first at $\omega > 1$, it does not vanish in the limit. This phenomenon has been discussed at length in ref. [11].

What may be surprising is that this extra contribution, required by gauge invariance, when considered in the limit $\omega \rightarrow 1$, exhibits a pure area dependence on its own, being the same no matter the orientation of the loop. Namely, the geometrical arguments (invariance under area-preserving diffeomorphism) which lead to a pure area dependence in two dimensions, but not in higher ones, are recovered in the limit $\omega \rightarrow 1$, in spite of the singular nature of this limit, and of the difference in the two results (with and without self-energy diagrams).

We consider this point quite intriguing; it seems that, in order to get beyond two dimensions towards higher ones, the theory needs further inputs which cannot be *a priori* guessed in two dimensions. On the other hand it is known that operators exist which are irrelevant at $\omega > 1$, but can be competitive in exactly two dimensions [18].

Our result can therefore be interpreted as a warning when one tries to extend straightforwardly conclusions obtained in strictly two dimensions to more realistic situations.

Before concluding let us summarize the main perturbative features which are common to both Feynman and light-cone gauges.

For $D > 2$ the $\mathcal{O}(g^4)$ result depends on the contour: if it has lightlike sides, there is a dependence only on the area, no matter the value of D . If instead the contour is a space-time rectangle, for $D > 2$ there is also a dependence on the ratio $\beta \equiv L/T$, still reproducing the expected exponential behaviour in the limit $T \rightarrow \infty$ ($\beta = 0$).

The limit $D \rightarrow 2$ of such $\mathcal{O}(g^4)$ result is finite and depends only on the area, no matter the orientation and the shape of the contour. It consists of two addenda (compare eq.(27) with eq.(13) of [11]).

In light cone gauge the second addendum comes from ‘crossed’ diagrams, the first one is due to the self-energy correction to the gluon propagator. In axial gauges the transverse degrees of freedom are coupled with a strength of order $D - 2$; nevertheless they produce a finite contribution when matching the self-energy loop singularity precisely at $D = 2$.

In exactly 1+1 dimensions therefore the first addendum is missing and one just gets the result of refs. [15] and [16]. Its area dependence is hardly surprising in view of the symmetry under area preserving diffeomorphisms at $D = 2$; it is perhaps remarkable that also the first addendum, which originates at $D > 2$, exhibits in the limit $D \rightarrow 2$ a pure area dependence on its own. However both contributions contain the factor $C_F C_A$ and thereby disagree with the simple area exponentiation. At a perturbative level there is a discontinuity, which is not surprising in the light of the arguments presented in ref. [16]; however it does not explain why agreement with the simple area behaviour is not recovered.

Moreover, the authors of ref. [16], working in exactly 1+1 dimensions, have succeeded in resumming the perturbative series: the result they get does not exhibit the usual purely exponential area law. Besides the appearance of Laguerre polynomials, the coefficient in the exponent multiplying the area is different from the usual one. We are thereby faced with a discrepancy.

Now we want to discuss the consequences concerning ALTE in the large- T limit. We have checked that our findings at $\mathcal{O}(g^4)$ comply with ALTE, as long as $\omega > 1$. At $\omega = 1$ this is not the case; however it is likely that ALTE in this case is restored by genuine non perturbative contributions, reconciling gauge invariance with basic spectral properties and solving the paradox.

As a matter of fact the usual $D = 2$ well established result can most safely be obtained by means of non perturbative techniques. Actually one could also get it by resumming the perturbative series, but only in axial gauges with a peculiar prescription for the propagator (the Cauchy principal value, which is doubtful in $D = 2$ and certainly incorrect for $D > 2$). The reason why this happens might be deep and related to peculiar properties of the $D = 2$

light-front vacuum in light-front quantization.

At a non-perturbative level there are arguments which show that at large N and on the sphere S_2 a phase transition occurs, induced by instantons (see ref. [19]). The purely exponential area behaviour occurs only in the strong coupling phase, which is dominated by instantons. In the weak coupling phase the result is completely different and agrees (after decompactification) with the ones of refs. [15] and [16]. This is the reason why we believe that the discrepancy can be solved by taking instantons into account [20]; they obviously do not contribute to any perturbative calculation, even when the perturbative series is fully resummed.

One could say that perturbative results are irrelevant at $D = 2$. We cannot share this opinion. At $D > 2$ perturbative results are the only easily accessible ones; several perturbative tests of gauge invariance have been performed in the past at $D > 2$, just *assuming* the simple area exponentiation in the large T -limit. One of the results of this paper is to prove that indeed at $D > 2$ such an exponentiation occurs as expected.

We do not think it is immaterial to understand how these nice features behave in the transition $D \rightarrow 2$, also in order to contrast them against genuine non perturbative results.

Why genuinely non perturbative contributions, which are likely to be relevant also in higher dimensions, are crucial only in two dimensions to possibly recover ALTE, is at present unknown. This very interesting issue is under investigation and will be discussed elsewhere.

APPENDIX A: EXCHANGE DIAGRAMS

In order to get the $\mathcal{O}(g^4)$ contribution to the Wilson Loop arising from the exchange diagrams, we only have to evaluate the maximally non Abelian diagrams, that in the present case are the so called crossed diagrams. In fact, the contribution coming from planar diagrams can be easily obtained through the Abelian exponentiation theorem, as explained in the main text. In this appendix we shall give the main sketch of computation of the seven independent crossed diagrams needed:

$$C_{(13)(13)} = \int_{-1}^1 du \int_{-1}^1 dv \frac{\alpha T^4}{[4L^2 - (u+v)^2 T^2 + i\epsilon]^{\omega-1}} \int_u^1 dt \int_v^1 ds \frac{1}{[4L^2 - (t+s)^2 T^2 + i\epsilon]^{\omega-1}}, \quad (A1)$$

$$C_{(24)(24)} = \int_{-1}^1 du \int_{-1}^1 dv \frac{\alpha L^4}{[L^2(u+v)^2 - 4T^2 + i\epsilon]^{\omega-1}} \int_u^1 dt \int_v^1 ds \frac{1}{[L^2(t+s)^2 - 4T^2 + i\epsilon]^{\omega-1}}, \quad (A2)$$

$$C_{(13)(24)} = \int_{-1}^1 du \int_{-1}^1 dv \frac{(-\alpha L^2 T^2)}{[L^2(u+v)^2 - 4T^2 + i\epsilon]^{\omega-1}} \int_{-1}^1 dt \int_{-1}^1 ds \frac{1}{[4L^2 - (t+s)^2 T^2 + i\epsilon]^{\omega-1}}, \quad (A3)$$

$$C_{(11)(13)} = \int_{-1}^1 du \int_{-1}^1 dv \frac{(-2\alpha T^4)}{[4L^2 - (u+v)^2 T^2 + i\epsilon]^{\omega-1}} \int_{-1}^u dt \int_u^1 ds \frac{1}{[-(t-s)^2 T^2 + i\epsilon]^{\omega-1}}, \quad (A4)$$

$$C_{(22)(24)} = \int_{-1}^1 du \int_{-1}^1 dv \frac{(-2\alpha L^4)}{[L^2(u+v)^2 - 4T^2 + i\epsilon]^{\omega-1}} \int_{-1}^u dt \int_u^1 ds \frac{1}{[(t-s)^2 L^2 + i\epsilon]^{\omega-1}}, \quad (A5)$$

$$C_{(11)(11)} = \int_{-1}^1 dt \int_t^1 du \int_u^1 ds \int_s^1 dv \frac{(2\alpha T^4)}{[-(t-s)^2 T^2 + i\epsilon]^{\omega-1} [-(u-v)^2 T^2 + i\epsilon]^{\omega-1}}, \quad (A6)$$

$$C_{(22)(22)} = \int_{-1}^1 dt \int_t^1 du \int_u^1 ds \int_s^1 dv \frac{(2\alpha L^4)}{[(t-s)^2 L^2 + i\epsilon]^{\omega-1} [(u-v)^2 L^2 + i\epsilon]^{\omega-1}}, \quad (A7)$$

where $\alpha = [\Gamma(\omega - 1)]^2 / (16\pi^{2\omega})$. As an example, we report the main sketch of computation of $C_{(13)(13)}$.

In order to perform the integrations a series expansion of the denominators in (A1) is not enough as the series do not converge in the entire integration domains. The necessary analytic continuations are provided by two Mellin-Barnes transformations:

$$\begin{aligned} C_{(13)(13)} = & \alpha T^4 (4L^2)^{2-2\omega} \frac{1}{[\Gamma(\omega - 1)]^2} \frac{1}{(2\pi i)^2} \int_{-i\infty}^{+i\infty} dy \Gamma(\omega - 1 + y) \Gamma(-y) \left(\frac{1}{-\beta^2 - i\epsilon} \right)^y \times \\ & \int_{-i\infty}^{+i\infty} dz \Gamma(\omega - 1 + z) \Gamma(-z) \left(\frac{1}{-\beta^2 - i\epsilon} \right)^z \times \\ & \int_{-1}^1 du \int_{-1}^1 dv \left| \frac{u+v}{2} \right|^{2y} \int_u^1 dt \int_v^1 ds \left| \frac{s+t}{2} \right|^{2z}, \end{aligned} \quad (A8)$$

where the path of integration over z is chosen in such a way that the poles of the function $\Gamma(\omega - 1 + z)$ lie to the left of the path of integration and the poles of the function $\Gamma(-z)$ lie to the right of it (the same for the integration over y).

After the integration over s, t, v and u we have the following expression:

$$\begin{aligned}
C_{(13)(13)} = & \alpha T^4 (4L^2)^{2-2\omega} \frac{1}{[\Gamma(\omega-1)]^2} \frac{1}{(2\pi i)^2} \int_{-i\infty}^{+i\infty} dy \Gamma(\omega-1+y) \Gamma(-y) \left(\frac{1}{-\beta^2 - i\epsilon} \right)^y \times \\
& \int_{-i\infty}^{+i\infty} dz \Gamma(\omega-1+z) \Gamma(-z) \left(\frac{1}{-\beta^2 - i\epsilon} \right)^z \times \\
& \frac{2^5}{(2z+1)(2z+2)} \left[\frac{1}{(2y+1)(2y+2)} - \frac{1}{(2y+1)(2y+2z+4)} \right. \\
& \left. + \frac{1}{(2y+2z+3)(2y+2z+4)} - \frac{\Gamma(2z+3)\Gamma(2y+1)}{\Gamma(2z+2y+5)} \right]. \tag{A9}
\end{aligned}$$

Then one has to integrate over z and y ; the integration contours have to be suitably chosen: for instance, in the present example, in order to apply Jordan's lemma, the integration paths must be closed with half-circles lying in the half planes $\text{Re}z < 0$ and $\text{Re}y < 0$. These integrations produce several double power series in the variable β^2 with finite convergence radii, which are particularly suited for a large T (small β) expansion. For instance, the last term in the square bracket of eq. (A9) gives the following contribution

$$\begin{aligned}
& \alpha T^4 (4L^2)^{2-2\omega} \frac{1}{[\Gamma(\omega-1)]^2} \frac{1}{(2\pi i)^2} \int_{-i\infty}^{+i\infty} dy \Gamma(\omega-1+y) \Gamma(-y) \left(\frac{1}{-\beta^2 - i\epsilon} \right)^y \\
& \times \int_{-i\infty}^{+i\infty} dz \Gamma(\omega-1+z) \Gamma(-z) \left(\frac{1}{-\beta^2 - i\epsilon} \right)^z \frac{2^5}{(2z+1)(2z+2)} \left[-\frac{\Gamma(2z+3)\Gamma(2y+1)}{\Gamma(2z+2y+5)} \right] \\
& = \frac{(2T)^{4-4\omega}}{\pi^{2\omega}} (LT)^2 \left\{ e^{-2i\pi\omega} \beta^{-2} \left(-\frac{1}{8} \right) \left(\frac{\pi}{\sin(\pi\omega)} \right)^2 \frac{\Gamma^2(\frac{3}{2}-\omega)}{\Gamma(\frac{1}{2})\Gamma(\frac{9}{2}-2\omega)\Gamma(5-2\omega)} \right. \\
& \times F_4(2\omega - \frac{7}{2}, 2\omega - 4, \omega - \frac{1}{2}, \omega - \frac{1}{2}; \beta^2, \beta^2) + e^{-i\pi\omega} \beta^{1-2\omega} \frac{i}{4\sin(\pi\omega)} \frac{\pi}{\Gamma(\frac{1}{2})\Gamma(\frac{3}{2}-\omega)\Gamma(\omega - \frac{3}{2})} \\
& \times F_4(\omega - \frac{5}{2}, \omega - 2, \omega - \frac{1}{2}, \frac{5}{2} - \omega; \beta^2, \beta^2) + e^{-i\pi\omega} \beta^{2-2\omega} \frac{1}{4\sin(\pi\omega)} \Gamma(\frac{1}{2}) \\
& \times \sum_{l=0}^{\infty} \sum_{m=0}^{\infty} \frac{\Gamma(m+1)\Gamma(l+m+\omega - \frac{3}{2})\Gamma(l+m+\omega - 2)}{\Gamma(l+\omega - \frac{1}{2})\Gamma(m+3-\omega)\Gamma(m+\frac{3}{2})} \frac{(\beta^2)^l}{l!} \frac{(\beta^2)^m}{m!} + \beta^{4-4\omega} \frac{\Gamma^2(\omega - \frac{3}{2})\Gamma^2(\frac{1}{2})}{4} \\
& \left. + i\beta^{5-4\omega} \Gamma(\frac{1}{2})\Gamma(\omega-2)\Gamma(\omega - \frac{3}{2}) - \frac{\beta^{6-4\omega}}{2} \left[\frac{1}{2}\Gamma^2(\frac{1}{2})\Gamma(\omega - \frac{3}{2})\Gamma(\omega - \frac{5}{2}) + \Gamma^2(\omega-2) \right] \right\} \tag{A10}
\end{aligned}$$

with the notations as in [21].

Repeating this procedure for each integral (A1)-(A7), one eventually recover eq. (19).

As a check of our calculations, we have explicitly verified the Abelian exponentiation theorem. The sum of all the crossed diagrams, which are proportional to $C_F^2 - (1/2)C_F C_A$, behaves like $(LT)^2 T^{4-4\omega}$, and therefore is depressed in the large T limit as long as $\omega > 1$. This means that only planar diagrams should contribute to the Abelian exponentiation in the large T limit. As a matter of fact this is in fact what happens: there is a single planar diagram that, alone, provides the dominant term for the Abelian exponentiation; it is the one in Fig. (2a). It can be checked that for such a diagram the leading term in the large T expansion is $(-1/2\pi^{2\omega})((2L)^{4-4\omega}(C_F LT)^2(\Gamma(\omega - 3/2)\Gamma(1/2))^2$, which is precisely the half of the square of the corresponding leading order of the sum of the single exchange diagrams.

APPENDIX B: BUBBLE DIAGRAMS

The complete one loop propagator (including ghost interaction) is given by

$$D_{\mu\nu}^{(2)ab} = \delta^{ab} \frac{g^2 C_A}{16\pi^{2\omega}} \frac{(1-3\omega)(2-\omega)(3-2\omega)\Gamma(1-\omega)\Gamma^2(\omega)\Gamma(2\omega-4)}{\Gamma(2\omega)\Gamma(4-\omega)(-x^2+i\epsilon)^{2\omega-3}} \times \left[\frac{x_\mu x_\nu}{(-x^2+i\epsilon)} - g_{\mu\nu} \frac{2\omega-5}{2(3-2\omega)} \right]. \quad (B1)$$

Writing explicitly all the possible bubble diagrams B_{ij} , it is not difficult to realize that $B_{11} = B_{33}$, $B_{22} = B_{44}$, $B_{12} = B_{34}$, $B_{14} = B_{23}$. In addition, the two last pairs of bubbles are in turn equal after a trivial change of variables, so that eq. (21) follow. The five independent bubbles are then

$$B_{11} = \int_{-1}^1 ds \int_{-1}^1 dt \frac{(\sigma T^2)}{[-(s-t)^2 T^2 + i\epsilon]^{2\omega-3}} \left[\frac{2\omega-1}{2(3-2\omega)} \right], \quad (B2)$$

$$B_{22} = \int_{-1}^1 ds \int_{-1}^1 dt \frac{(\sigma L^2)}{[(s-t)^2 L^2 + i\epsilon]^{2\omega-3}} \left[\frac{1-2\omega}{2(3-2\omega)} \right], \quad (B3)$$

$$B_{13} = \int_{-1}^1 ds \int_{-1}^1 dt \frac{(-\sigma T^2)}{[-(s+t)^2 T^2 + 4L^2 + i\epsilon]^{2\omega-3}} \left[\frac{(s+t)^2 T^2}{4L^2 - (s+t)^2 T^2 + i\epsilon} - \frac{2\omega-5}{2(3-2\omega)} \right], \quad (B4)$$

$$B_{24} = \int_{-1}^1 ds \int_{-1}^1 dt \frac{(-\sigma L^2)}{[(s+t)^2 L^2 - 4T^2 + i\epsilon]^{2\omega-3}} \left[\frac{(s+t)^2 L^2}{(s+t)^2 L^2 - 4T^2 + i\epsilon} + \frac{2\omega-5}{2(3-2\omega)} \right], \quad (B5)$$

$$B_{12} = \int_{-1}^1 ds \int_{-1}^1 dt \frac{\sigma L^2 T^2 (t-1)(s+1)}{[(s+1)^2 L^2 - T^2 (t-1)^2 + i\epsilon]^{2\omega-2}}, \quad (B6)$$

where

$$\sigma = \frac{g^4 C_F C_A}{16\pi^{2\omega}} \frac{(3\omega-1)(2-\omega)(3-2\omega)\Gamma(1-\omega)\Gamma^2(\omega)\Gamma(2\omega-4)}{\Gamma(2\omega)\Gamma(4-\omega)} \quad (B7)$$

Again, integration can be performed using Mellin-Barnes techniques leading to

$$\begin{aligned} \mathcal{W}^{(2)} = & \frac{C_F C_A (2L)^{4-4\omega} (LT)^2 \Gamma^2(\omega) (3\omega-1) \Gamma(1-\omega) \Gamma(2\omega-2)}{2\pi^{2\omega} \Gamma(2\omega) \Gamma(4-\omega)} \times \\ & \left\{ e^{-2i\pi\omega} \beta^{4\omega-6} \left[\frac{(2\omega-1)}{(4\omega-6)} \frac{1-(4\omega-7)(1-\beta^2)^{4-2\omega} + (4\omega-8) {}_2F_1(2\omega-3, 2\omega-7/2; 2\omega-5/2; \beta^2)}{(2\omega-4)(4\omega-7)} \right. \right. \\ & - \frac{2\omega-1}{(4\omega-6)(2\omega-4)} [{}_2F_1(2\omega-4, -1/2; 1/2; \beta^2) - 1] + \frac{1}{2\omega-3} [{}_2F_1(2\omega-3, -1/2; 1/2; \beta^2) - 1] \\ & + \frac{1}{(2\omega-4)(2\omega-3)} [(1-\beta^2)^{4-2\omega} - 1] \left. \right] \\ & + e^{-2i\pi\omega} \beta^{4\omega-4} \frac{2(2\omega-3) {}_2F_1(2\omega-2, 2\omega-5/2; 2\omega-3/2; \beta^2) - (4\omega-5)(1-\beta^2)^{3-2\omega}}{(2\omega-3)(4\omega-5)} \\ & \left. + i\beta \frac{(\omega-3)\Gamma(1/2)\Gamma(2\omega-7/2)}{\Gamma(2\omega-2)} + \beta^2 \frac{3-\omega}{(\omega-2)(4\omega-7)} \right\}. \end{aligned} \quad (B8)$$

By performing the large T limit in eq. (B8) one arrives at eq. (22).

APPENDIX C: SPIDER DIAGRAMS

The spider diagrams are by far the most complicated to evaluate. The sum of the 6 inequivalent spider diagrams, with the appropriate weights, is given by

$$\begin{aligned} \mathcal{W}^{(3)} = & 2(S_{124} + S_{123} + S_{122} + S_{144} + S_{112} + S_{114}) \equiv \\ & \frac{C_F C_A \Gamma(2\omega-2) L^2 T^{6-4\omega}}{32\pi^{2\omega}} \int_0^1 d\rho_1 \int_0^1 d\rho_2 \int_0^1 d\rho_3 \delta(1-\rho_1-\rho_2-\rho_3) (\rho_1 \rho_2 \rho_3)^{\omega-2} \times \\ & \left\{ \int_{-1}^1 ds_1 \int_{-1}^1 ds_2 \int_{-1}^1 ds_3 (\rho_1(\rho_1-1) + \rho_2(\rho_2-1) - 2\rho_1\rho_2 + (\rho_2-\rho_1)s_3\rho_3) \times \right. \\ & [(\rho_1-\rho_2-s_3\rho_3)^2 - \beta^2(s_1\rho_1-s_2\rho_2+\rho_3)^2 - \rho_1(1-\beta^2 s_1^2) - \rho_2(1-\beta^2 s_2^2) - \rho_3(s_3^2-\beta^2) + i\epsilon]^{2-2\omega} \\ & + \int_{-1}^1 ds_1 \int_{-1}^1 ds_2 \int_{-1}^1 ds_3 (\rho_1(\rho_1-1) + \rho_3(\rho_3-1) - 2\rho_1\rho_3 + (\rho_1-\rho_3)s_2\rho_2) \times \\ & [(s_1\rho_1-\rho_2-s_3\rho_3)^2 - \beta^2(\rho_1+s_2\rho_2-\rho_3)^2 - \rho_1(s_1^2-\beta^2) - \rho_2(1-\beta^2 s_2^2) - \rho_3(s_3^2-\beta^2) + i\epsilon]^{2-2\omega} \\ & + \int_{-1}^1 ds_1 \int_{-1}^{s_1} ds_2 \int_{-1}^1 ds_3 (\rho_1(\rho_1-1) - \rho_2(\rho_2-1) + (\rho_1-\rho_2)s_3\rho_3) \times \\ & [(\rho_1+\rho_2+s_3\rho_3)^2 - \beta^2(s_1\rho_1+s_2\rho_2-\rho_3)^2 - \rho_1(1-s_1^2\beta^2) - \rho_2(1-\beta^2 s_2^2) - \rho_3(s_3^2-\beta^2) + i\epsilon]^{2-2\omega} \end{aligned}$$

$$\begin{aligned}
& + \int_{-1}^1 ds_1 \int_{-1}^{s_1} ds_2 \int_{-1}^1 ds_3 (\rho_1(1-\rho_1) + \rho_2(\rho_2-1) + (\rho_1-\rho_2)s_3\rho_3) \times \\
& [(\rho_1+\rho_2-s_3\rho_3)^2 - \beta^2(s_1\rho_1+s_2\rho_2+\rho_3)^2 - \rho_1(1-s_1^2\beta^2) - \rho_2(1-\beta^2s_2^2) - \rho_3(s_3^2-\beta^2) + i\epsilon]^{2-2\omega} \\
& + \int_{-1}^1 ds_1 \int_{-1}^1 ds_2 \int_{-1}^{s_2} ds_3 (\rho_2(1-\rho_2) + \rho_3(\rho_3-1) + (\rho_2-\rho_3)s_1\rho_1) \times \\
& [(\rho_1+s_2\rho_2+s_3\rho_3)^2 - \beta^2(s_1\rho_1-\rho_2-\rho_3)^2 - \rho_1(1-s_1^2\beta^2) - \rho_2(s_2^2-\beta^2) - \rho_3(s_3^2-\beta^2) + i\epsilon]^{2-2\omega} \\
& + \int_{-1}^1 ds_1 \int_{-1}^1 ds_2 \int_{-1}^{s_2} ds_3 (\rho_2(\rho_2-1) + \rho_3(1-\rho_3) + (\rho_2-\rho_3)s_1\rho_1) \times \\
& [(\rho_1-s_2\rho_2-s_3\rho_3)^2 - \beta^2(s_1\rho_1+\rho_2+\rho_3)^2 - \rho_1(1-s_1^2\beta^2) - \rho_2(s_2^2-\beta^2) - \rho_3(s_3^2-\beta^2) + i\epsilon]^{2-2\omega} \}
\end{aligned}$$

The above integrals can be more conveniently grouped as

$$\mathcal{W}^{(3)} = \frac{C_F C_A (LT)^2 (2T)^{4-4\omega}}{\pi^{2\omega}} e^{-2i\pi\omega} [I_1(\beta^2) + I_2(\beta^2) + I_3(\beta^2) + I_4(\beta^2)] \quad (C1)$$

where

$$\begin{aligned}
I_1(\beta^2) &= \Gamma(2\omega-3) 2^{4\omega-10} \int_0^1 [d\rho] \int_{-1}^1 [ds] (\rho_1\rho_2\rho_3)^{\omega-2} \frac{\rho_1-\rho_2}{\rho_1+\rho_2} \frac{\partial}{\partial s_3} \\
& [P_1^{3-2\omega} + \theta(s_1-s_2)P_2^{3-2\omega} + \theta(s_1-s_2)P_3^{3-2\omega}] \\
I_2(\beta^2) &= \Gamma(2\omega-3) 2^{4\omega-10} \int_0^1 [d\rho] \int_{-1}^1 [ds] (\rho_1\rho_2\rho_3)^{\omega-2} \frac{\rho_2-\rho_1}{\beta^2(\rho_1+\rho_2)} \frac{\partial}{\partial s_3} \\
& [P_4^{3-2\omega} + \theta(s_1-s_2)P_5^{3-2\omega} + \theta(s_1-s_2)P_6^{3-2\omega}] \\
I_3(\beta^2) &= -\Gamma(2\omega-2) 2^{4\omega-7} \int_0^1 [d\rho] \int_{-1}^1 [ds] (\rho_1\rho_2\rho_3)^{\omega-2} \frac{\rho_1\rho_2}{\rho_1+\rho_2} P_1^{2-2\omega} \\
I_4(\beta^2) &= -\Gamma(2\omega-2) 2^{4\omega-7} \int_0^1 [d\rho] \int_{-1}^1 [ds] (\rho_1\rho_2\rho_3)^{\omega-2} \frac{\rho_1\rho_2}{\rho_1+\rho_2} P_4^{2-2\omega} \quad (C2)
\end{aligned}$$

where $[ds] = ds_1 ds_2 ds_3$, $[d\rho] = d\rho_1 d\rho_2 d\rho_3 \delta(1-\rho_1-\rho_2-\rho_3)$ and

$$\begin{aligned}
P_1 &= (\rho_1-\rho_2+s_3\rho_3)^2 - \beta^2(s_1\rho_1-s_2\rho_2-\rho_3)^2 - \rho_1(1-s_1^2\beta^2) - \rho_2(1-\beta^2s_2^2) - \rho_3(s_3^2-\beta^2) + i\epsilon \\
P_2 &= (\rho_1+\rho_2+s_3\rho_3)^2 - \beta^2(s_1\rho_1+s_2\rho_2-\rho_3)^2 - \rho_1(1-s_1^2\beta^2) - \rho_2(1-\beta^2s_2^2) - \rho_3(s_3^2-\beta^2) + i\epsilon \\
P_3 &= (\rho_1+\rho_2-s_3\rho_3)^2 - \beta^2(s_1\rho_1+s_2\rho_2+\rho_3)^2 - \rho_1(1-s_1^2\beta^2) - \rho_2(1-\beta^2s_2^2) - \rho_3(s_3^2-\beta^2) + i\epsilon \\
P_4 &= (s_1\rho_1-s_2\rho_2-\rho_3)^2 - \beta^2(\rho_1-\rho_2+s_3\rho_3)^2 - \rho_1(s_1^2-\beta^2) - \rho_2(s_2^2-\beta^2) - \rho_3(1-s_3^2\beta^2) + i\epsilon \\
P_5 &= (s_1\rho_1+s_2\rho_2+\rho_3)^2 - \beta^2(\rho_1+\rho_2-s_3\rho_3)^2 - \rho_1(s_1^2-\beta^2) - \rho_2(s_2^2-\beta^2) - \rho_3(1-s_3^2\beta^2) + i\epsilon \\
P_6 &= (s_1\rho_1+s_2\rho_2-\rho_3)^2 - \beta^2(\rho_1+\rho_2+s_3\rho_3)^2 - \rho_1(s_1^2-\beta^2) - \rho_2(s_2^2-\beta^2) - \rho_3(1-s_3^2\beta^2) + i\epsilon
\end{aligned}$$

As already anticipated in the main text, the above integrals have not been evaluated exactly. However, the leading power of T is just the factor $T^{6-4\omega}$ contained in the overall constant, as can be easily realized by the fact that the integrals I_1, \dots, I_4 are finite when evaluated for $\beta = 0$. In turn, only $I_1(\beta^2 = 0)$ and $I_3(\beta^2 = 0)$ can be evaluated analytically, whereas for $I_2(\beta^2 = 0)$ and $I_4(\beta^2 = 0)$ we have only an expansion around $\omega = 1$ that, however, is just what we need. The results are

$$\begin{aligned}
I_1(\beta^2 = 0) &= \frac{\Gamma(2\omega - 2)}{3 - 2\omega} \left[\frac{\Gamma(\omega)\Gamma(\omega + 1)}{\omega(\omega - 2)^2\Gamma(2\omega - 1)} - \frac{\pi}{(2\omega - 4)\sin(\pi\omega)} \right] \\
I_2(\beta^2 = 0) &= -\frac{1}{4(\omega - 1)^2} + \frac{\gamma - 1/2}{2(\omega - 1)} \\
&\quad + \frac{17}{4} + \frac{1}{2}\gamma(1 - \gamma) + \frac{7}{24}\pi^2 - \pi^2\log 2 - \frac{3}{2}\zeta(3) + \mathcal{O}(\omega - 1) \\
I_3(\beta^2 = 0) &= \frac{2}{\Gamma(5 - 2\omega)} \left[\Gamma(2\omega - 2)\Gamma(1 - \omega)\Gamma(3 - \omega) + \frac{\pi}{\sin(\pi\omega)} \times \right. \\
&\quad \left. \sum_{n=1}^{\infty} \frac{1}{n!} \left(\frac{\Gamma(2\omega - 2 + n)\Gamma(3 + n - \omega)}{(2n + 1)\Gamma(n + \omega)} - \frac{\Gamma(n + \omega - 1)\Gamma(4 - 2\omega + n)}{(2n + 3 - 2\omega)\Gamma(2 - \omega + n)} \right) \right] \\
I_4(\beta^2 = 0) &= -\frac{1}{2(\omega - 1)^2} + \frac{\gamma - 4}{(\omega - 1)} + \\
&\quad + 8\gamma - \gamma^2 - 22 + \frac{\pi^2}{12} + \pi^2\log 2 + \frac{3}{2}\zeta(3) + \mathcal{O}(\omega - 1)
\end{aligned} \tag{C3}$$

By expanding I_1 and I_3 one can easily get eq. (25).

REFERENCES

- [1] A. M. Polyakov, Phys. Lett. 82B, 247 (1972);
 J. B. Kogut and L. Susskind, Phys. Rev. D11, 395 (1975).
- [2] W. Fishler, Nucl. Phys. B129, 157 (1977).
- [3] K. Wilson, Phys. Rev. D10, 2445 (1974);
 L.S. Brown and W.I. Weisberger, *ibid* 20, 3239 (1979).
- [4] G. 't Hooft, Nucl. Phys. B75, 461 (1974).
- [5] C.G. Callan, N. Coote and D.J. Gross, Phys. Rev. D 13, 1649 (1976).
- [6] T.T. Wu, Phys. Lett. 71B, 142 (1977).
- [7] S. Mandelstam, Nucl. Phys. B213, 149 (1983);
 G. Leibbrandt, Phys. Rev. D29, 1699 (1984).
- [8] A. Bassutto, M. Dalbosco, I. Lazzizzera and R. Soldati, Phys. Rev. D31, 2012 (1985).
- [9] A. Bassutto, M. Dalbosco and R. Soldati, Phys. Rev. D36, 3138 (1987).
- [10] A. Bassutto, G. Nardelli and R. Soldati, *Yang–Mills theories in algebraic non covariant gauges* (World Scientific, Singapore, 1991).
- [11] A. Bassutto, F. De Biasio and L. Griguolo, Phys. Rev. Lett. 72, 3141 (1994).
- [12] I.A. Korchemskaya and G.P. Korchemsky, Phys. Lett. B 287, 169 (1992).
- [13] A. Bassutto, I.A. Korchemskaya, G.P. Korchemsky and G. Nardelli, Nucl. Phys. B 408, 62 (1993).
- [14] S. Caracciolo, G. Curci and P. Menotti, Phys. Lett. 113B, 311 (1982);
 J.P. Leroy, J. Micheli and G.C. Rossi, Nucl. Phys. B232, 511 (1984).
- [15] A. Bassutto, D. Colferai and G. Nardelli, Nucl. Phys. B501, 227 (1997) and E. *ibid* 507, 746 (1997).

- [16] M. Staudacher and W. Krauth, Phys. Rev. D57, 2456 (1998).
- [17] J. Frenkel and J. C. Taylor, Nucl. Phys. B246, 231 (1984).
- [18] E. Witten, Commun. Math. Phys. 141, 153 (1991);
M.R. Douglas, K. Li and M. Staudacher, Nucl. Phys. B420, 118 (1994).
- [19] M.R. Douglas and V.A. Kazakov, Phys. Lett. B319, 219 (1993);
D.V. Boulatov, Mod. Phys. Lett. A9, 365 (1994);
D.J. Gross and A. Matytsin, Nucl. Phys. B429, 50 (1994).
- We thank L. Griguolo for calling our attention to these papers.
- [20] A. Bassutto and L. Griguolo, hep-th/9806037.
- [21] *Higher Trascendental Functions*, Vol. 1, Ed. A. Erdélyi, McGraw-Hill , New York 1953.

FIGURES

FIG. 1. Parametrization of the closed rectangular loop γ in four segments γ_i .

FIG. 2. Example of non-crossed and crossed diagrams.

FIG. 3. Examples of crossed diagrams; they are labelled as $C_{(13)(13)}$, $C_{(11)(11)}$ and $C_{(13)(11)}$, respectively

FIG. 4. The three crossed diagrams that are unrelated to other diagrams through symmetry relations; they are $C_{(13)(13)}$, $C_{(24)(24)}$ and $C_{(13)(24)}$.

FIG. 5. Examples of bubble diagrams. They are labelled as B_{11} , B_{13} and B_{34} , respectively.

FIG. 6. Examples of spider diagrams. They are labelled as S_{123} , S_{112} , respectively.

Fig. 1

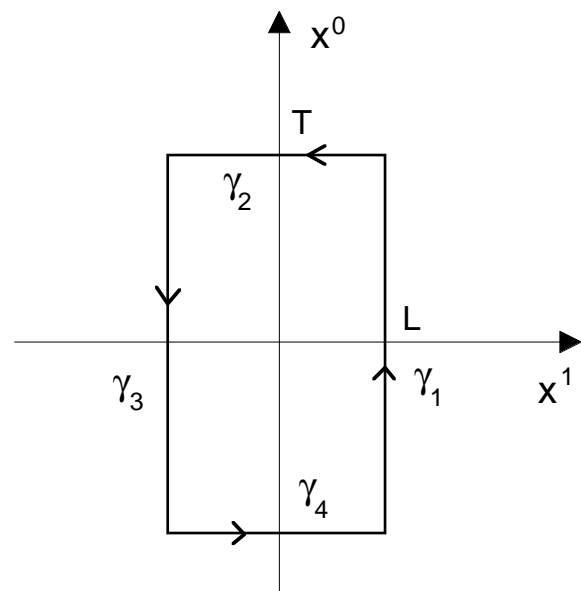


Fig. 2



Fig. 3

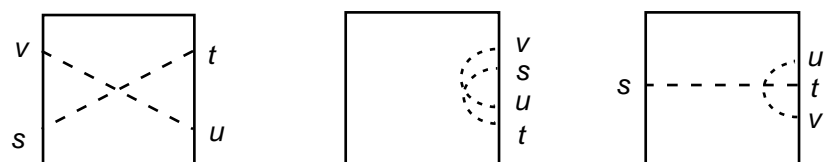


Fig. 4

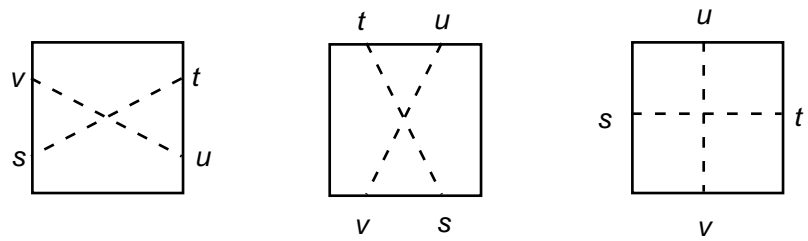


Fig. 5

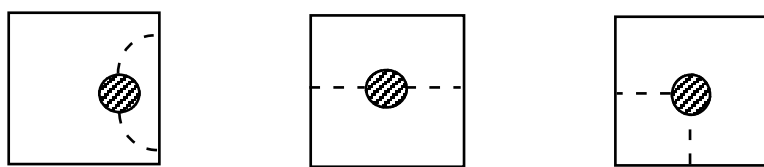


Fig. 6

